



A new approach in photocatalytic degradation of tetracycline using biogenic zinc oxide nanoparticles and peroxymonosulfate under UV_C irradiation

Mohammad Malakootian^{a,b}, Seyedeh Nastaran Asadzadeh^{c,*}, Mohsen Mehdipoor^{a,b}, Davood Kalantar-Neyestanaki^d

^aEnvironmental Health Engineering Research Center, Kerman University of Medical Sciences, Kerman, Iran, emails: m.malakootian@yahoo.com (M. Malakootian), mmehdipoor@yahoo.com (M. Mehdipoor)

^bDepartment of Environmental Health, School of Public Health, Kerman University of Medical Sciences, Kerman, Iran

^cStudent Research Committee, School of Public Health, Kerman University of Medical Sciences, Kerman, Iran, Tel. +98 (343) 2315700; Fax: +98 (343) 32315700; email: snasadzadeh3@gmail.com

^dDepartment of Microbiology and Virology, School of Medicine, Kerman University of Medical Science, Kerman, Iran, email: Davoud1362@gmail.com

Received 26 June 2020; Accepted 30 January 2021

ABSTRACT

Refractory and non-biodegraded pollutants such as antibiotics are the major threat to humans and the environment. Integrating several kinds of advanced oxidation processes into one system such as UV/ZnO/PMS (PMS – peroxymonosulfate) process has been proposed to be an efficient strategy for removing pollutants from the environment at a low-cost. In this study, zinc oxide (ZnO) nanoparticles were, firstly, synthesized and showed super reactivity as well as good reusability for tetracycline degradation in the integrated UV/PMS process from the aqueous system. To describe the structure and morphology of the nanoparticles, UV-Visible spectroscopy, X-ray diffraction, and transmission electron microscopy were used. The results demonstrated 95.6% degradation occurred under the condition of pH = 7.0, PMS = 2 mM, 2 g L⁻¹ ZnO, and 90 min reaction time. First-order kinetics was fitted for UV/ZnO/PMS with the rate constant of 0.018 min⁻¹. PMS exhibited superiority to other electron acceptors (persulfate and hydrogen peroxide). Scavenger's experiments confirmed the presence of both sulfate and hydroxyl radicals in the degradation process. The systematic condition experiments further verified the dual functionality of the biogenic ZnO nanoparticles system, in which PMS activator for tetracycline molecule oxidation under ultraviolet irradiation and actively played the role of a photocatalyst.

Keywords: Photocatalysis; Peroxymonosulfate; Tetracycline; Biogenic zinc oxide nanoparticles

1. Introduction

Antibiotics are widely used as human and animal drugs to treat microbial infections [1]. About 30%–80% of antibiotics are not metabolized in the human and animal body and rather are excreted in the urine and feces as active compounds [2,3]. Pharmaceutical compounds enter the aquatic environment from sources such as the

pharmaceutical industry, hospital effluents, human and livestock feces, wastewater treatment effluents, and laboratory and research activities [4]. Some of the adverse effects of antibiotics entering the human body include increased bacterial resistance, genotoxicity, and gastrointestinal disorders [5]. Conventional wastewater treatment, on the other hand, removes only 60%–90% of antibiotics [6]. Therefore, these agents are found in surface water, groundwater,

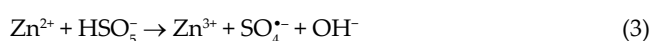
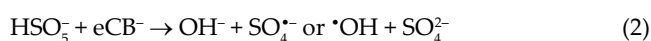
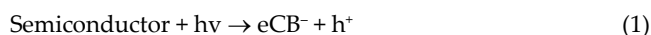
* Corresponding author.

wastewater, soil, and sediment [7,8]. Tetracycline (TC) antibiotics are the second most commonly used antibiotics worldwide for the production and use of antibiotics that are frequently used today to treat a variety of infectious diseases [9]. The presence of this antibiotic in the environment poses a threat to human health and ecosystem function [10]. Therefore, an efficient system for eliminating these compounds is essential.

Methods used to remove antibiotics from aqueous and wastewater environments include membrane processes [11], adsorption [12], physical [13], biological processes [14], advanced oxidation including UV [15], ultrasound [16], ozonation [17], and synthetic methods such as MWCNT/TiO₂ [18]. Among the above methods, advanced oxidation processes (AOPs) provide an effective way of decomposing hazardous and biodegradable pollutants in aquatic environments [19]. Removal of pollutants in the advanced oxidation process is based on some chemical oxidants (e.g., H₂O₂, PMS, and O₃) by free radicals such as hydroxyl and sulfate radicals. These radicals have a high oxidation potential that is capable of mineralizing many organic and toxic compounds [20,21].

In addition, the advanced oxidation processes have advantages such as process simplicity, low-cost, high efficiency, and complete degradation of pollutants [22,23].

Recently, peroxymonosulfate as a new oxidant has been the subject of intense research because of advantages such as the stability, safety, the higher redox potential of corresponding intermediate sulfate radicals (SO₄^{•-}; 2.5–3.1 V, [•]OH: 1.8–2.7 V) with a longer lifetime, and strong oxidation ability [24,25]. In addition, this oxidant is easily activated by heat [26], ultraviolet light [27], alkaline [28], ultrasound [29], and proper transitional metal ions (Fe²⁺, Zn²⁺, Mn²⁺) [30–32].



The use of catalysts in photocatalytic processes increases the rate of radical production [33–40], reaction rate, and efficiency [41]. Using various semiconductor materials (e.g., TiO₂, ZnO, CuO, and MgO) [42,43], metallic or metallic oxides reinforced (e.g., CuO/SnO₂, TiO₂/Al₂O₃, and CuO/ZnO) [44], and some porous materials (e.g., activated carbon granules and zeolites) [45] have been widely used to eliminate contaminants in water and wastewater treatment. Among the advanced oxidation methods, semiconductor-based photocatalytic processes such as ZnO have received much attention because of their high efficiency and easy application [46,47].

Zinc oxide (ZnO) is known as an excellent semiconductor material with a wide-direct bandgap (3.37eV), large exciton binding energy (60 MeV), non-toxic and stable photochemical properties [48].

The photocatalytic activity of ZnO has two major features: (i) its bandwidth of ZnO is wide, which leads to only

absorbing ultraviolet light but not completing using the visible light, and (ii) ZnO material has a high recombination rate of electron-hole pairs [38,49].

The activation of peroxymonosulfate by ultraviolet and ZnO catalysts and the production of hydroxyl and sulfate radicals for the decomposition of TC are explained by Eqs. (1)–(4).

In this study, the biogenic ZnO NPs synthesized using an extract of palm kernel, then we aimed to report the performance of UV/biogenic ZnO NPs in the presence of peroxymonosulfate (PMS) for TC removal with a focus on the main operating parameters such as pH, PMS, TC concentration and catalyst dosages. Also, the photo-degraded samples were analyzed by the chemical oxygen demand (COD) analysis. Finally, the quenching experiments were conducted for determining the mechanism of TC degradation in the photocatalysis process.

2. Material and methods

2.1. Materials

TC powder with 98% purity was prepared from Sigma-Aldrich Co., (USA) to perform photocatalytic decomposition. The antibiotic characteristics are presented in Table 1 [2]. Hydrogen peroxide (30%), sodium hydroxide (NaOH), and sulfuric acid (96%) (H₂SO₄) were obtained from Merck Company. (Germany) Peroxymonosulfate (2KHSO₅·KHSO₄·K₂SO₄; OXONE) and zinc nitrate (99% pure) were provided by Sigma-Aldrich (USA). All the applied chemical reagents were of analytical grade and without being further purified before use. All used solutions were prepared with highly pure DI-water.

2.2. Preparation of extract and biosynthesis of zinc oxide

The pits of date palm were collected from the City of Bam in Kerman Province in Southeastern Iran in 2020.

First, 20 g of pits were disinfected by 3% sodium hypochlorite for 3 min and then washed with distilled water 3 times and each time was 2 min. Then the seeds were disinfected with 70% alcohol for 2 min and then washed 3 times with distilled water and each time was 2 min. Then sterile water was added with the ratio of 10:1 (10 mL of water per 1 g of seed), they were placed in the dark for 2 d at 25°C. After 2 d, the liquid phase was filtered with Whatman No. 1 and the obtained filtered extract was used for the synthesized nanoparticles. Zinc nitrate were used at concentrations of 0.1, 0.25, 0.5, 0.75, and 1 mM for biosynthesis of zinc oxide nanoparticles. Thus, 10 mL of the extract was added to 90 mL of nitrate-zinc solution with mentioned concentrations separately (while zinc nitrate was not added to the control sample). The treated extracts were incubated at 70°C for 2 h. Lastly, the solution was calcinated for 4 h at 400°C to obtained white powder.

2.3. Characterization techniques

The absorption spectra of ZnO NPs were recorded by a Shimadzu UV 2600 spectrophotometer (Japan).

The surface morphology of the samples (ZnO NPs) was observed employing a transmission electron microscopy

(TEM) field. In addition, X-ray diffraction (XRD) analysis with Cu K α radiation ($\lambda = 0.154$ nm) was also performed to show the crystallinity and phase composition of the samples (Philips XRD, Model: PW1730, Holland).

2.4. Analytical methods

The TC concentration in the solutions was measured using a high-performance liquid chromatography (HPLC) (Model KNAUER) device equipped with the ultimate variable wavelength UV detector. The calibration curve was produced at five levels (ranging from 1 to 50 mg L⁻¹) for the TC quantification.

The mineralization of TC was evaluated by measuring the COD using the dichromatic closed reflux method.

The TC removal efficiency under both adsorption and oxidation systems was determined via Eq. (5):

$$R(\%) = TC_0 - \frac{TC_t}{TC_0} \times 100 \quad (5)$$

where TC_0 and TC_t (mg L⁻¹) are the TC concentrations in aqueous media at time 0 and t (min), respectively [3].

2.5. Photocatalytic activity of ZnO NPs

All photocatalysis experiments were conducted in a quartz cylindrical reactor (500 mL) containing 200 mL of TC solution under ambient laboratory conditions. Initially, by dissolving TC hydrochloride salt of more than 98% purity (C₂₂H₂₄N₂O₈·HCl) in distilled water, TC stock solution (200 mg L⁻¹) was prepared weekly and kept in the dark at 4°C. The pH of the solution was adjusted by H₂SO₄ and NaOH (0.1 N).

In the next step, a certain amount of ZnO was added to the solution and then a certain amount of PMS as an electron acceptor was introduced to the solution. A mechanical stirrer was applied for mixing the solution. The temperature of the solution was kept in a range of 22°C–24°C.

One low-pressure UV_C lamp (6 W, Philips, 254–258 nm) was used as a UV source for light irradiation, which was placed above the reactor with a distance of 2 cm. Photocatalytic process experiments were carried out for a period of 90 min. About 2 mL of the sample from the solution was extracted at selected time intervals and during the reaction. The samples were finally filtered using a 0.22 μ m syringe filter before injection to HPLC for measuring the residue of TC.

All experiments were conducted in triplicate and average values were used in the results. The efficiency of the photocatalytic process was studied as a function of pH and various concentrations of catalyst, PMS, and TC. The kinetics of TC degradation by UV/ZnO/PMS was studied in the next step.

3. Results and discussion

3.1. UV-Vis, TEM, and XRD analysis on ZnO NPs

The UV-Vis spectrum of the prepared biogenic ZnO NPs is described in Fig. 1a. The sharp absorption peak observed at 360–380 nm confirms the formation of ZnO

NPs by the auto combustion method [49]. In addition, there was no other peak observed in the spectrum except for the characteristic peak, which indicates that ZnO NPs prepared using palm kernel possess high purity.

A transmission electron microscopy (TEM) was used to identify the shape and size of ZnO nanoparticles [50]. The average particle size of synthesized nanoparticles was 50 nm. Fig. 1b shows that particle size was 50 nm; hence, the particle size distribution was appropriate. The as-prepared precursor ZnO was approximately spherical and oval as TEM patterns are shown in Fig. 1b.

XRD analysis was used to approve the crystal structure and purity of ZnO nanoparticles [51]. XRD patterns were drawn to represent the crystallinity of the nanoparticles as well as phase identification (Fig. 1c).

XRD spectrum of ZnO nanoparticles (Fig. 2) showed the absorption peaks at angles of 31.4°, 35.2°, 57.8°, 63.4°, 72.1°, and 76.4° degrees which are linked to surfaces at levels of (100), (102), (103), (200), (004), and (202), respectively. Thus the spectrum clearly shows that the ZnO nanoparticles are biosynthesized by a natural source.

3.2. Effect of operating parameters on the photocatalytic degradation of TC

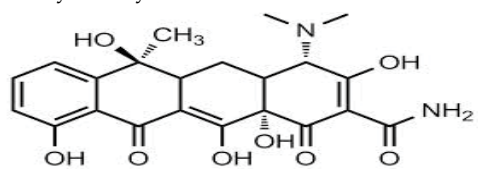
3.2.1. Effect of pH

The photocatalytic activity is greatly influenced by the surface charge properties of the materials, the molecular charge, the adsorption of organic molecules onto the photocatalyst surfaces, and the number of hydroxyl and sulfate radicals produced [52]. The effect of changing pH from 5 to 11 for the initial solution under the initial antibiotic concentration of 10 mg L⁻¹, 4 mM peroxymonosulfate dose, and ZnO 3 g L⁻¹ catalyst dose under UV irradiation at room temperature (25°C) is shown in Fig. 2a. The results showed that photocatalytic decomposition and constant decomposition rate increased with increasing pH. This result can be explained by the different properties of TCs and ZnO at different pH values.

The zero-point charge of ZnO is 9.0 ± 0.3 . Therefore, ZnO levels are positive at pH < 9 and negative at pH > 9. Here, TC showed different species at different pHs [53]. It was obvious that a larger number of negative TCH⁻ species would form instead of zwitterion TCH²⁻ when pH varies from 5.0 to 9.0. On the other hand, a positively charged ZnO surface would attract more TCH⁻ molecules, leading to a faster trend of TCs photodegradation rate. Both TC species (TC²⁻) and ZnO were negatively charged when pH was increased to 11.0, followed by a declined degradation rate due to the repulsive force between TC²⁻ and ZnO. However, the reason for the maximum rate at this pH was likely the large quantities of OH⁻ ions on the ZnO surface, which favored the formation of \cdot OH radicals and subsequently the hydrolysis of TCs [16,29].

The TC removal reached 86.7% and 81.4% at pH values of 11.0 and 7.0, respectively. Considering the low-efficiency distinction and the amount of alkali dosage, 7.0 was chosen as the appropriate pH because of the similarity to the neutral environment, which makes it suitable in a real degradation process without pre-adjustment of pH.

Table 1
Chemical properties of tetracycline hydrochloride (TC)

Properties	Tetracycline hydrochloride
Structure	
Chemical formula	$C_{22}H_{24}O_8N_2$
Molecular weight ($g\ mol^{-1}$)	444.435
λ_{max}	261 nm
Solubility (mg/mL)	10

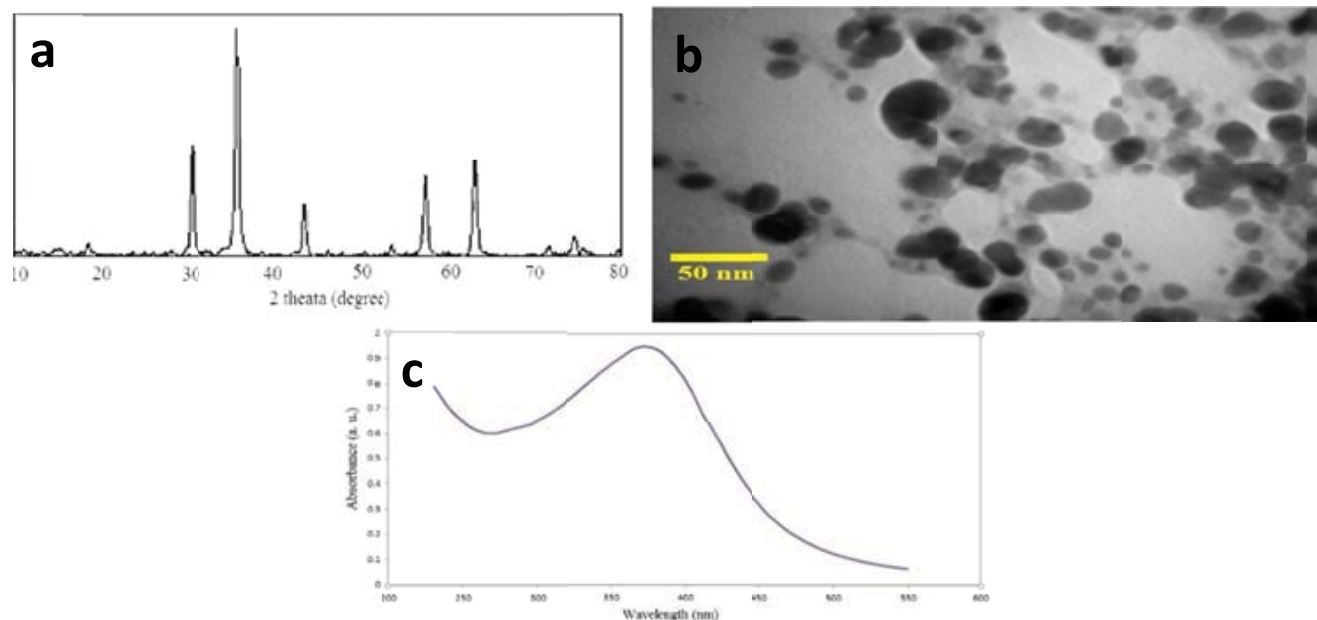


Fig. 1. UV-Vis absorption spectra (a), transmission electron microscopy (TEM) image (b), X-ray diffraction (XRD) pattern (c) of the synthesized biogenic ZnO nanoparticles (NPs).

During the use of PMS as an oxidant, in addition to the radical production of sulfate, it plays an important role in producing organic compounds due to the higher oxidation potential of organic compounds [54]. This reagent, as expressed by Eq. (6), can affect the hydroxyl water molecules and convert them to hydroxyl radicals [55]. These radicals, in turn, can play a role in the acidic conditions of sulfate ions, which are converted into free radicals of sulfate. Therefore, in neutral and basic pH values, the $SO_4^{\bullet-}$ is converted to $\bullet OH$ according to Eqs. (7) and (8), leading to an increase in oxidation and removal efficiency [56].

The initial pH of the antibiotic solution also affects the adsorption of organic compounds on the photocatalyst surface [57]. Accordingly, pH = 7 was selected as the optimum pH.



3.2.2. Effect of photocatalyst dosage

The effect of the initial concentration of the catalyst on the efficiency of the photocatalytic process (concentration range of 0.5–3 $g\ L^{-1}$) was investigated under the following conditions: initial concentration of TC 10 $mg\ L^{-1}$, 4 mM PMS dose, and optimum pH 7. The rate of photocatalytic degradation of TC antibiotics increased with increasing catalyst dose (up to 2 $g\ L^{-1}$) and then decreased. The higher the photocatalyst dose, the more active sites are found on the surface of the photocatalyst, which promotes hydroxyl radical production [58].

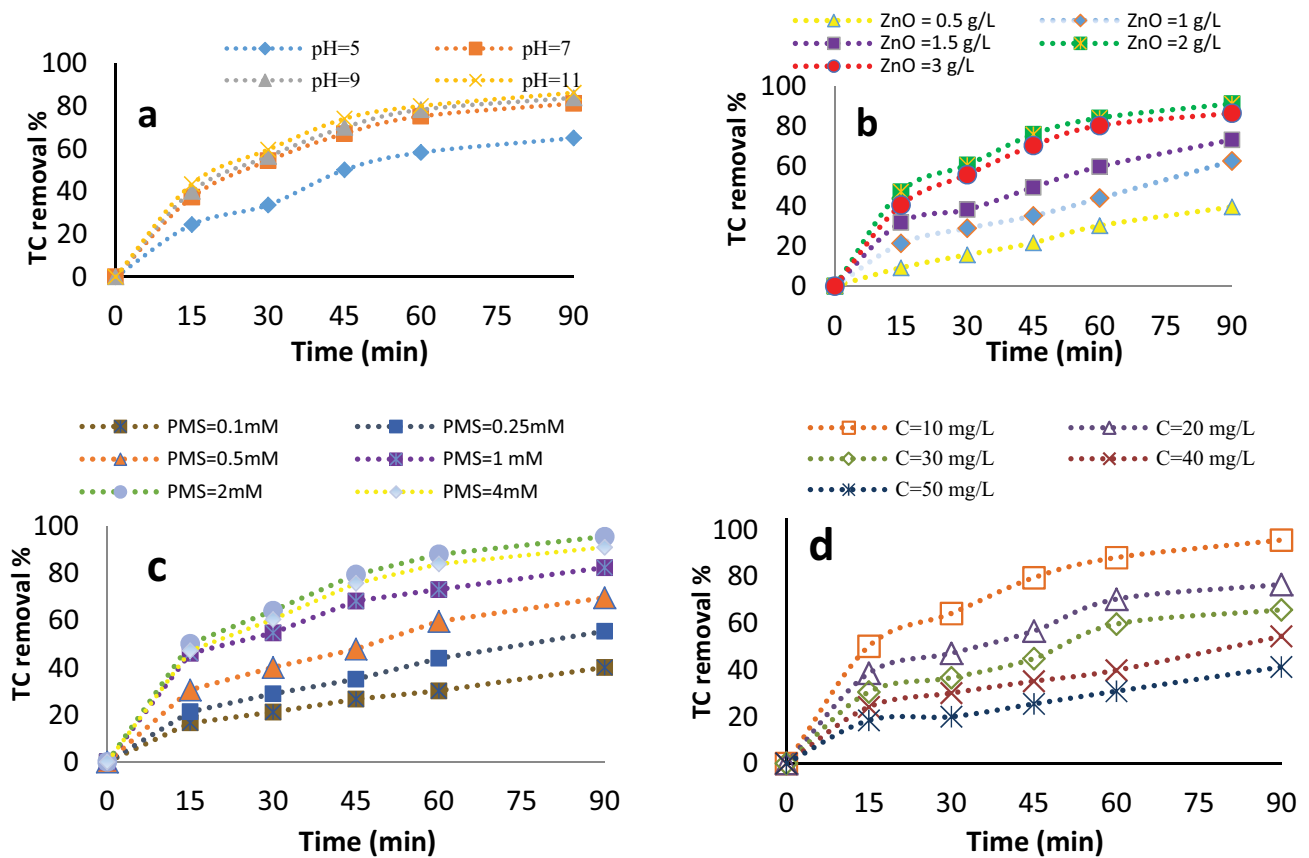
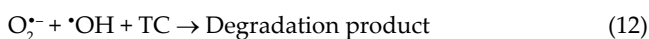
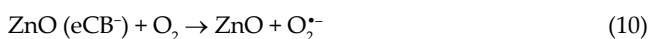
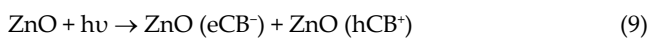


Fig. 2. Effects of pH (a), biogenic ZnO dosage (b), PMS concentration (c), and TC concentration (d) on the removal efficiency of tetracycline.

In the photocatalytic oxidation process, the photo-excited ZnO and an electron-hole pair form as follows (Eqs. (9)–(11)) [59]:

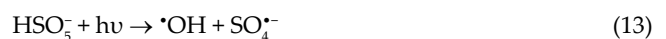


Hydroxyl and $\text{O}_2^{\cdot-}$ radicals substituted radicals react with antibiotics to form the final products [Eq. (12)]. However, increasing the catalyst dose more than the optimum value reduces the process efficiency because the excess amount of catalyst reduces the penetration of light through the protective effect of the suspended particles [60].

The deactivation of all initiated molecules by a crash with molecules in the ground state controls the reaction and thus reduces the rate of reaction. In addition, the screening effect of the aggregation of catalyst particles can prevent photons from reaching the inner surface of the catalyst. In other words, the decrease in TC transported to the ZnO surface lowers the removal rate between $\cdot\text{OH}$ and TC [61].

3.2.3. Effect of PMS concentration

To investigate different oxidant concentrations, PMS experiments with different initial oxidant concentrations of 0.1 to 4 mM were performed. Peroxomonosulfate was used to produce hydroxyl and sulfate radicals and thereby aiding in the oxidation of TC [Eq. (13)] [59]. Furthermore, peroxomonosulfate was converted by transition metals such as ZnO to hydroxyl and sulfate radicals, which can cause antibiotic degradation [Eq. (14)] [62]. The production of sulfate, hydroxyl, and electron-hole pair radicals increased with increasing peroxomonosulfate from 0.1 to 2 mM, leading to an increase in the TC removal efficiency from 40.1% to 95.6%.



However, increasing the PMS concentration above 2 mM significantly decreased the removal efficiency, which can be attributed to several factors. The observed decrease in the removal efficiency beyond the optimum peroxomonosulfate concentration (2 mM) can be caused by the recombination of excess hydroxyl radicals, resulting in hydrogen peroxide molecule productions because these molecules are less reactive compared with hydroxyl radicals and act as a radical scavenger [62].

Another reason for this role of scavenger radical sulfate at high doses is that additional amounts of PMS compete with TC to react with radical sulfate, which reduces the available radicals [Eq. (15)] [63]. In addition, excess sulfate radicals are known to obstruct ZnO_{surf} e^- of the catalyst, which could induce consumption of $\text{SO}_4^{\bullet-}$ at a higher concentration of the oxidant [Eq. (16)] [64].



3.2.4. Effect of initial TC concentration

The effect of initial antibiotic concentration on its degradation was investigated with different concentrations of TC from 10 to 50 mg L^{-1} . The ZnO dosage, PMS concentration, and initial pH values were 2 g L^{-1} , 2 mM, and 7, respectively.

As shown in Fig. 2d the rate of photocatalytic degradation at low initial concentrations is higher than that of high initial concentrations [65].

The TC degradation efficiencies were 41% and 95% for the initial concentrations of 10 and 50 mg L^{-1} , respectively. At high concentrations of TC, high adsorption of organic molecules on the surface of the catalyst prevents the absorption of heat and energy produced by ultraviolet waves. Therefore, low concentrations of TC should be used to enhance the efficiency of the photocatalytic process for antibiotic degradation. The amount of TC degradation depends on the probability of hydroxyl radical formation on the catalyst surfaces and the probability of the hydroxyl radical reaction with TC [16]. In the photocatalytic processes, the active surface of the catalyst available for the reaction plays a significant role. As the antibiotic concentration increases, the active surfaces of the catalyst and the length of the photon pathway to the solution decrease. Therefore, when the ZnO surface is coated with TC, the production of hydroxyl radicals is not sufficient. As a result, the amount of photocatalytic degradation decreases with increasing the TC concentration [66].

3.3. Estimation of COD

COD is used as an efficient method to measure organic wastewater. In this experiment, the oxygen required for the oxidation of organic materials to carbon dioxide and water was measured (Fig. 3). In chemical oxidation processes, organic contaminants may be converted to smaller molecules with less toxicity than the primary molecule. COD parameter is used to determine the level of degradation of antibiotics. COD was measured at 0, 30, 60 and 90 min following the photocatalytic process and reached 180, 96, 71 and 60 mg L^{-1} , respectively. A decrease in the COD over time indicates the mineralization of antibiotics to non-toxic compounds [18,67].

3.4. Stability of photocatalyst ZnO

The practical applications for the photocatalysts require excellent properties such as the maintaining of recyclability and high photocatalytic activity.

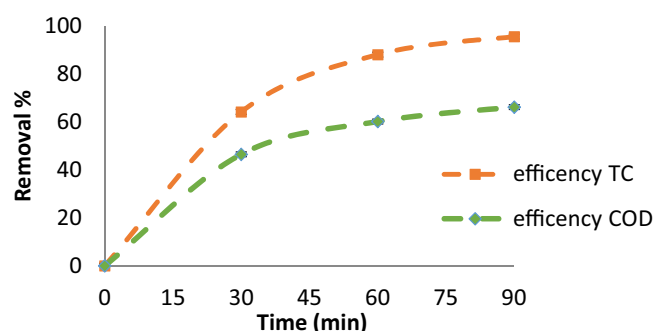


Fig. 3. Mineralization of tetracycline investigated using measuring the COD in UV/PMS/ZnO systems: ZnO NPs = 2 g L^{-1} ; PMS = 2 mM; TC = 10 mg L^{-1} ; initial pH = 7.

Therefore, the stability of ZnO photocatalysts with TC photocatalytic degradation recovery experiments in the presence of peroxymonosulfate and UV irradiation was examined at pH 7, 2 g L^{-1} catalysts, 2 mM PMS, and 10 mg L^{-1} TC. In this experiment, the photocatalyst was removed by centrifugation after each cycle and then washed with distilled water and ethanol and dried in an oven at 100°C. The sample was then reused for subsequent decomposition. As observed, the degradation efficiency of TC decreased from 95.6% to 91.7% after 90 min of reuse (Fig. 4).

Also, the photocatalytic activity of the samples only minimally decreased due to the unavoidable loss of photocatalysts during the cycle processes [68,69]. The decrease in removal efficiency is due to the retention of TC-mediated byproducts on the catalyst surface and the reduction of the interaction between peroxymonosulfate with ZnO and ultimately the reduction of radical production [70].

The reasons for the reduction in removal efficiency can be due to (1) the loss of the ZnO species mass on the catalyst surface during consecutive runs; (2) the intermediate products of TC degradation remaining in the catalyst hindered the degradation reaction; and (3) the residual (unreacted) TC adsorbed on the catalyst surface inhibited the interaction of ZnO and PMS, which decreased the production of reactive radicals [60].

3.5. Mechanism of photodegradation

In this work, quenching tests were carried out to determine the reactive species that formed and contributed to TC degradation over UV/PMS/ZnO process.

The factors such as bandgap energy, the oxidation state of the dopant, and the recombination of the photo-generated electron-hole pairs may be taken into the consideration for the improved photocatalytic properties of doped ZnO [71].

Generally, the mechanism of photocatalytic degradation occurs in two main stages: (1) the adsorption of pollutant molecules onto the surfaces of the photocatalysts and (2) the degradation of pollutants. For this reason, TC is first adsorbed onto the catalyst layer to form a relatively stable complex. When photocatalytic nanoparticles are illuminated under UV stimulation, ZnO nanoparticles can absorb light and produce electron/hole pairs [72].

The mechanism of photocatalytic degradation requires the identification of reactive species in the process.

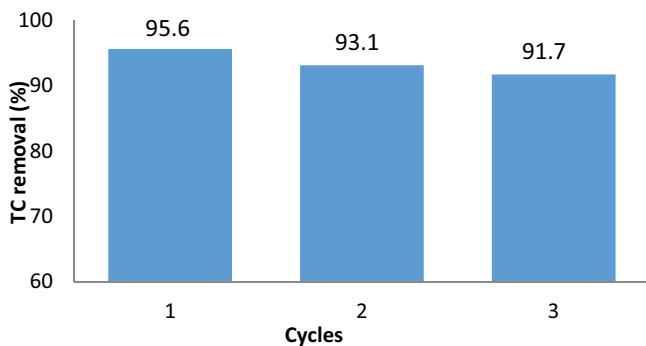


Fig. 4. Recyclability of ZnO nanoparticles for tetracycline removal in the UV/PMS/ZnO systems: ZnO NPs = 2 g L⁻¹; PMS = 2 mM; TC = 10 mg L⁻¹; initial pH = 7.

Photocatalytic degradation of TC by zinc oxide was examined using ethanol (EtOH) and tert-butanol (TBA) under optimum conditions (pH 7, 2 g L⁻¹ catalyst, 2 mM PMS, and 10 mg L⁻¹ TC). TBA is an effective compound for scavenging the hydroxyl radical with a second-order rate constant of 3.8–7.6 × 10⁸ M⁻¹ s⁻¹ while its second-order rate constant for sulfate radical is approximately 1,000 folds less compared to hydroxyl radical. Besides, EtOH has proved as a strong scavenger for both the radicals with second-order rate constants of 1.6–7.7 × 10⁷ and 1.2–2.8 × 10⁹ M⁻¹ s⁻¹ for sulfate radical and hydroxyl radical, respectively [73,74].

The results of photocatalysis experiments conducted in the presence of these scavengers (with a concentration of 0.1 N) in the UV_λ/ZnO/PMS process are presented in Fig. 5. As can be seen, in the presence of EtOH, the degradation efficiency was significantly reduced (66.4%) such that in the presence of TBA, the removal efficiency was 84.19%. These results indicate that the sulfate radical has a higher contribution to the degradation of TC than the hydroxyl radical.

3.6. Removal efficiency of antibiotic in different systems

A comparison of different processes helps to understand the mechanism and function of the photocatalytic process and to determine the role of each parameter for TC decomposition. Table 2 shows the TC decomposition in different processes. The results indicate that UV and PMS alone have no significant effect on TC degradation; on the other hand, TC is very stable against oxidant and UV radiation alone. Furthermore, UV radiation alone cannot activate PMS for TC degradation; the PMS is not easily decomposed under UV radiation [75].

The removal efficiency of photolysis alone was found to be only 8.3% because only a few amounts of •OH radicals are formed in the presence of UV alone.

Almost no TC removal efficiency was observed by ZnO alone, reflecting that the adsorption effect of the catalyst is negligible in the performed condition. The high adsorption efficiency is attributed to the large ZnO surface area [76]. Also, PMS alone and UV/PMS processes cannot produce significant free radicals. The UV/ZnO process, however, significantly increased the degradation efficiency because the photocatalysts produce a significant amount of

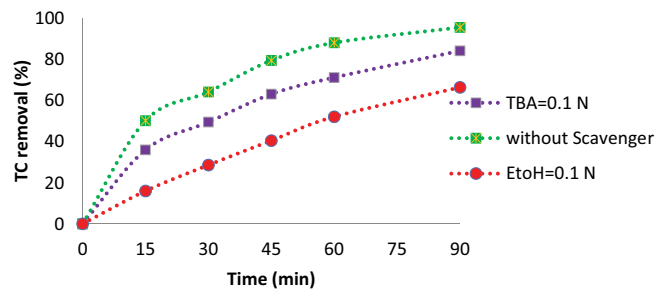


Fig. 5. Effects of radical scavengers (TBA and EtOH) tetracycline removal in the UV/PMS/ZnO systems: ZnO NPs = 2 g L⁻¹; PMS = 2 mM; TC = 10 mg L⁻¹; initial pH = 7.

Table 2

Removal efficiency of antibiotic in different systems: ZnO NPs = 2 g L⁻¹; PMS = 2 mM; TC = 10 mg L⁻¹; initial pH = 7

Process	Removal efficiency %
UV	8.3
PMS	12.8
ZnO	45.8
UV/PMS	20.19
PMS/ZnO	68.9
UV/ZnO	50.14
UV/PMS/ZnO	95.6

hydroxyl free radicals for antibiotic decomposition in the presence of UV irradiation [77]. ZnO/PMS showed high activity for PMS activation. UV/ZnO in the presence of PMS increased the decomposition rate from 50.14% to 95.6%. PMS has two essential roles in increasing the degradation rate:

First, the SO₄^{•-} produced on the ZnO surface from PMS under ultraviolet waves directly degrades TC molecules in the solution. Second, HSO₅⁻ acts as an electron acceptor and inhibits electron-hole pair recombination, allowing more •OH to be produced [78].

3.7. Effect of other electron acceptors on the UV_λ/ZnO system

The performance of ZnO photocatalytic activity in the presence of other electron receptors was examined under optimal conditions (pH 7, 2 g L⁻¹ catalyst, and 10 mg L⁻¹ TC). Hydrogen peroxide, persulfate (PS), like PMS, was used in the UV_λ/ZnO process (Fig. 6). After 90 min, the removal rates TC for PMS, PS, and H₂O₂ oxidants in combination with UV and ZnO were found to be 95.6%, 92%, and 81.5%, respectively. From these results, it can be concluded that the synthesized catalyst has a very good catalytic activity for the decomposition of the three oxidants, but hydrogen peroxide has less degradation efficiency for the TC antibiotic.

Besides, persulfate and PMS had a similar trend in the degradation of TC. According to Eqs. (17) and (18), persulfate and hydrogen peroxide produced radical sulfate and hydroxyl, respectively [79]. The results showed that electron acceptor catalysis based on sulfate (such as PMS, PS) was more effective than hydrogen peroxide.

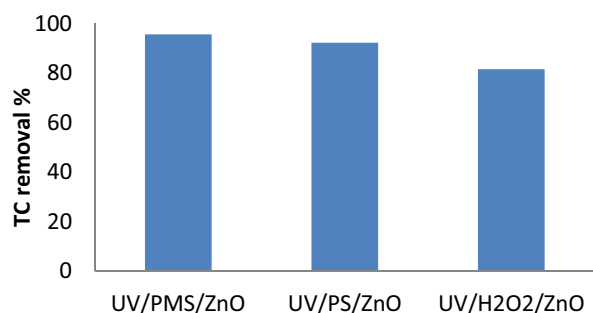


Fig. 6. Effect of other electronic receivers on the UV_c/ZnO system: ZnO NPs = 2 g L⁻¹; [PMS], [PS], [H₂O₂] = 2 mM; TC = 10 mg L⁻¹; initial pH = 7.



The generation of free radical species is intensified in the presence of PMS under an ultraviolet wave as shown in the following equation [74].



Sulfate radical (SO₄^{•-}) with high oxidation capability (up to 3.1 eV) and long half-life (up to 40 μs) can be considered as an effective alternative to ·OH for the decomposition of most refractory organic compounds [74]. The results of Duan's studies showed that in the photocatalytic processes based on radical sulfate, PMS was an effective oxidant for the decomposition of various pollutants [80].

3.8. Degradation kinetics

Kinetics of TC decomposition was examined using UV/ZnO/PMS process under optimum conditions (pH: 7, PMS concentration: 2 mM, TC concentration: 10 mg L⁻¹, and ZnO NPs dose: 2 g L⁻¹).

The pseudo-first-order and pseudo-second-order model equations are given as Eqs. (20) and (21), respectively [81].

$$\ln\left(\frac{C}{C_0}\right) = -k_1 t \quad (20)$$

$$\frac{1}{C} - \frac{1}{C_0} = -k_2 t \quad (21)$$

where C₀ represents the initial concentration and C_t the final concentration at time = t (mg L⁻¹).

The correlation coefficients (R²) for pseudo-first-order and pseudo-second-order kinetic models were obtained at 0.928 and 0.731, respectively. As can be seen, the kinetic model follows the pseudo-first-order model (Table 3).

The rate of TC decomposition was observed to be a function of time (x). The results are similar to those of

Table 3
Kinetic parameters for the TC degradation using the UV/ZnO/PMS process

C ₀ (mg L ⁻¹)	Pseudo-first-order		Pseudo-second-order	
	R ²	k ₁	R ²	k ₂
10	0.928	0.018	0.731	0.01

a study by Wan et al., who analyzed the degradation of TC in water using the US process [82].

4. Conclusion

In this study, the degradation of TC using the AOPs (UV/ZnO/PMS) process was studied. The effects of pH, PMS concentration, ZnO NPs dose, and initial TC concentration were examined on the degradation of TC. ZnO nanoparticles were successfully synthesized. The structural properties and particle size of ZnO nanoparticles were studied using XRD, TEM, and UV-Vis spectroscopy. The particle size average of ZnO nanoparticles was 50 nm.

The ZnO catalyst, in addition to its high reusability, showed excellent catalytic activity for the decomposition of PMS and the production of sulfate-free radicals.

Scavenger experiments showed that hydroxyl and sulfate radical had an effective role in the degradation of TC. Based on the results, it was found that the advanced oxidation using the UV/ZnO/PMS process could be considered as a suitable method for TC decomposition. The addition of ZnO NPs and PMS significantly increased the removal efficiency. Furthermore, the experimental data were in good agreement with a pseudo-first-order kinetic model.

Acknowledgment

This study was carried out in the Environmental Health Engineering Research Center of Kerman University of Medical Sciences and the Technology of Kerman University of Medical Sciences was sponsored. The authors take this opportunity to express their gratitude for the support and assistance extended by the facilitators during the conduct of the research.

References

- [1] B. Li, J. Ma, L. Zhou, Y. Qiu, Magnetic microsphere to remove tetracycline from water: adsorption, H₂O₂ oxidation and regeneration, *Chem. Eng. J.*, 330 (2017) 191–201.
- [2] M. Malakootian, S.N. Asadzadeh, Oxidative removal of tetracycline by sono Fenton-like oxidation process in aqueous media, *Desal. Water Treat.*, 193 (2020) 302–401.
- [3] M. Malakootian, S.N. Asadzadeh, Removal of tetracycline from aqueous solution by ultrasound and ultraviolet enhanced persulfate oxidation, *Desal. Water Treat.*, 197 (2020) 191–199.
- [4] R. Dagherir, P. Drogui, Tetracycline antibiotics in the environment: a review, *Environ. Chem. Lett.*, 11 (2013) 209–227.
- [5] E.S. Elmolla, M. Chaudhuri, Degradation of amoxicillin, ampicillin and cloxacillin antibiotics in aqueous solution by the UV/ZnO photocatalytic process, *J. Hazard. Mater.*, 173 (2010) 445–449.
- [6] V. Homem, L. Santos, Degradation and removal methods of antibiotics from aqueous matrices—a review, *J. Environ. Manage.*, 92 (2011) 2304–2347.

- [7] M.B. Ahmed, J.L. Zhou, H.H. Ngo, W. Guo, Adsorptive removal of antibiotics from water and wastewater: progress and challenges, *Sci. Total Environ.*, 532 (2015) 112–126.
- [8] I.R. Bautitz, R.F.P. Nogueira, Degradation of tetracycline by photo-Fenton process—solar irradiation and matrix effects, *J. Photochem. Photobiol., A*, 187 (2007) 33–39.
- [9] J.J. López-Peñalver, M. Sánchez-Polo, C.V. Gómez-Pacheco, J. Rivera-Utrilla, Photodegradation of tetracyclines in aqueous solution by using UV and UV/H₂O₂ oxidation processes, *J. Chem. Technol. Biotechnol.*, 85 (2010) 1325–1333.
- [10] H.M. Lwin, W. Zhan, S. Song, F. Jia, J. Zhou, Visible-light photocatalytic degradation pathway of tetracycline hydrochloride with cubic structured ZnO/SnO₂ heterojunction nanocatalyst, *Chem. Phys. Lett.*, 736 (2019) 136806, <https://doi.org/10.1016/j.cplett.2019.136806>.
- [11] C.F. Couto, L.C. Lange, M.C.S. Amaral, A critical review on membrane separation processes applied to remove pharmaceutically active compounds from water and wastewater, *J. Water Process Eng.*, 26 (2018) 156–175.
- [12] Y. Gao, Y. Li, L. Zhang, H. Huang, J. Hu, S.M. Shah, X. Su, Adsorption and removal of tetracycline antibiotics from aqueous solution by graphene oxide, *J. Colloid Interface Sci.*, 368 (2012) 540–546.
- [13] P.-H. Chang, Z. Li, T.-L. Yu, S. Munkhbayer, T.-H. Kuo, Y.-C. Hung, J.-S. Jean, K.-H. Lin, Sorptive removal of tetracycline from water by palygorskite, *J. Hazard. Mater.*, 165 (2009) 148–155.
- [14] D.I. Massé, N.M.C. Saady, Y. Gilbert, Potential of biological processes to eliminate antibiotics in livestock manure: an overview, *Animals*, 4 (2014) 146–163.
- [15] A.K. Biñ, S. Sobera-Madej, Comparison of the advanced oxidation processes (UV, UV/H₂O₂ and O₃) for the removal of antibiotic substances during wastewater treatment, *Ozone Sci. Eng.*, 34 (2012) 136–139.
- [16] R.D.C. Soltani, M. Mashayekhi, M. Naderi, G. Boczkaj, S. Jorfi, M. Safari, Sonocatalytic degradation of tetracycline antibiotic using zinc oxide nanostructures loaded on nano-cellulose from waste straw as nanosonocatalyst, *Ultrason. Sonochem.*, 55 (2019) 117–124.
- [17] P. Liu, H. Zhang, Y. Feng, F. Yang, J. Zhang, Removal of trace antibiotics from wastewater: a systematic study of nanofiltration combined with ozone-based advanced oxidation processes, *Chem. Eng. J.*, 240 (2014) 211–220.
- [18] M. Ahmadi, H.R. Motlagh, N. Jaafarzadeh, A. Mostoufi, R. Saeedi, G. Barzegar, S. Jorfi, Enhanced photocatalytic degradation of tetracycline and real pharmaceutical wastewater using MWCNT/TiO₂ nano-composite, *J. Environ. Manage.*, 186 (2017) 55–63.
- [19] M. Klavarioti, D. Mantzavinos, D. Kassinos, Removal of residual pharmaceuticals from aqueous systems by advanced oxidation processes, *Environ. Int.*, 35 (2009) 402–417.
- [20] E.A. Serna-Galvis, J. Silva-Agredo, A.L. Giraldo-Aguirre, O.A. Flórez-Acosta, R.A. Torres-Palma, High frequency ultrasound as a selective advanced oxidation process to remove penicillinic antibiotics and eliminate its antimicrobial activity from water, *Ultrason. Sonochem.*, 31 (2016) 276–283.
- [21] J. Jeong, W. Song, W.J. Cooper, J. Jung, J. Greaves, Degradation of tetracycline antibiotics: mechanisms and kinetic studies for advanced oxidation/reduction processes, *Chemosphere*, 78 (2010) 533–540.
- [22] Y. Zhang, Y. Zhuang, J. Geng, H. Ren, K. Xu, L. Ding, Reduction of antibiotic resistance genes in municipal wastewater effluent by advanced oxidation processes, *Sci. Total Environ.*, 550 (2016) 184–191.
- [23] G. Lofrano, R. Pedrazzani, G. Libralato, M. Carotenuto, Advanced oxidation processes for antibiotics removal: a review, *Curr. Org. Chem.*, 21 (2017) 1054–1067.
- [24] J. Cao, L. Lai, B. Lai, G. Yao, X. Chen, L. Song, Degradation of tetracycline by peroxymonosulfate activated with zero-valent iron: performance, intermediates, toxicity and mechanism, *Chem. Eng. J.*, 364 (2019) 45–56.
- [25] Q. Yang, X. Yang, Y. Yan, C. Sun, H. Wu, J. He, D. Wang, Heterogeneous activation of peroxymonosulfate by different ferromanganese oxides for tetracycline degradation: Structure dependence and catalytic mechanism, *Chem. Eng. J.*, 348 (2018) 263–270.
- [26] Y. Liu, Y. Wang, Q. Wang, J. Pan, J. Zhang, Simultaneous removal of NO and SO₂ using vacuum ultraviolet light (VUV)/heat/peroxymonosulfate (PMS), *Chemosphere*, 190 (2018) 431–441.
- [27] J. Sharma, I.M. Mishra, D.D. Dionysiou, V. Kumar, Oxidative removal of Bisphenol A by UV-C/peroxymonosulfate (PMS): kinetics, influence of co-existing chemicals and degradation pathway, *Chem. Eng. J.*, 276 (2015) 193–204.
- [28] B.-T. Zhang, W. Xiang, X. Jiang, Y. Zhang, Y. Teng, Oxidation of dyes by alkaline-activated peroxymonosulfate, *J. Environ. Eng.*, 142 (2016) 4016003.
- [29] R. Yin, W. Guo, H. Wang, J. Du, X. Zhou, Q. Wu, H. Zheng, J. Chang, N. Ren, Enhanced peroxymonosulfate activation for sulfamethazine degradation by ultrasound irradiation: performances and mechanisms, *Chem. Eng. J.*, 335 (2018) 145–153.
- [30] T. Zhang, H. Zhu, J.-P. Croue, Production of sulfate radical from peroxymonosulfate induced by a magnetically separable CuFe₂O₄ spinel in water: efficiency, stability, and mechanism, *Environ. Sci. Technol.*, 47 (2013) 2784–2791.
- [31] J. Du, J. Bao, Y. Liu, H. Ling, H. Zheng, S.H. Kim, D.D. Dionysiou, Efficient activation of peroxymonosulfate by magnetic Mn-MGO for degradation of bisphenol A, *J. Hazard. Mater.*, 320 (2016) 150–159.
- [32] F. Ghanbari, M. Moradi, Application of peroxymonosulfate and its activation methods for degradation of environmental organic pollutants, *Chem. Eng. J.*, 310 (2017) 41–62.
- [33] F. Tamaddon, A. Nasiri, G. Yazdanpanah, Photocatalytic degradation of ciprofloxacin using CuFe₂O₄@methyl cellulose based magnetic nanobiocomposite, *MethodsX*, 7 (2020) 100764, [doi: 10.1016/j.mex.2019.12.005](https://doi.org/10.1016/j.mex.2019.12.005).
- [34] M. Malakootian, M. Khatami, H. Mahdizadeh, A. Nasiri, M. Amiri Gharaghani, A study on the photocatalytic degradation of *p*-Nitroaniline on glass plates by thermo-immobilized ZnO nanoparticle, *Inorg. Nano-Metal Chem.*, 50 (2020) 124–135.
- [35] A. Nasiri, F. Tamaddon, M.H. Mosslemin, M. Faraji, A microwave assisted method to synthesize nanoCoFe₂O₄@methyl cellulose as a novel metal-organic framework for antibiotic degradation, *MethodsX*, 6 (2019) 1557–1563.
- [36] M. Malakootian, A. Nasiri, A. Asadipour, M. Faraji, E. Kargar, A facile and green method for synthesis of ZnFe₂O₄@CMC as a new magnetic nanophotocatalyst for ciprofloxacin removal from aqueous media, *MethodsX*, 6 (2019) 1575–1580.
- [37] F. Tamaddon, M.H. Mosslemin, A. Asadipour, M.A. Gharaghani, A. Nasiri, Microwave-assisted preparation of ZnFe₂O₄@methyl cellulose as a new nano-biomagnetic photocatalyst for photodegradation of metronidazole, *Int. J. Biol. Macromol.*, 154 (2020) 1036–1049.
- [38] M. Malakootian, A. Nasiri, A.N. Alibeigi, H. Mahdizadeh, M.A. Gharaghani, Synthesis and stabilization of ZnO nanoparticles on a glass plate to study the removal efficiency of acid red 18 by hybrid advanced oxidation process (Ultraviolet/ZnO/ultrasonic), *Desal. Water Treat.*, 170 (2019) 325–336.
- [39] M. Malakootian, A. Smith Jr., M.A. Gharaghani, H. Mahdizadeh, A. Nasiri, G. Yazdanpanah, Decoloration of textile Acid Red 18 dye by hybrid UV/COP advanced oxidation process using ZnO as a catalyst immobilized on a stone surface, *Desal. Water Treat.*, 182 (2020) 385–394.
- [40] H. Mahdizadeh, A. Nasiri, M.A. Gharaghani, G. Yazdanpanah, Hybrid UV/COP advanced oxidation process using ZnO as a catalyst immobilized on a stone surface for degradation of acid red 18 dye, *MethodsX*, 7 (2020) 101118, <https://doi.org/10.1016/j.mex.2020.101118>.
- [41] S. Sakthivel, B. Neppolian, M.V. Shankar, B. Arabindoo, M. Palanichamy, V. Murugesan, Solar photocatalytic degradation of azo dye: comparison of photocatalytic efficiency of ZnO and TiO₂, *Sol. Energy Mater. Sol. Cells*, 77 (2003) 65–82.
- [42] S. Chakrabarti, B.K. Dutta, Photocatalytic degradation of model textile dyes in wastewater using ZnO as semiconductor catalyst, *J. Hazard. Mater.*, 112 (2004) 269–278.

- [43] S. Chen, Y. Liu, Study on the photocatalytic degradation of glyphosate by TiO_2 photocatalyst, *Chemosphere*, 67 (2007) 1010–1017.
- [44] A. Samad, M. Furukawa, H. Katsumata, T. Suzuki, S. Kaneco, Photocatalytic oxidation and simultaneous removal of arsenite with CuO/ZnO photocatalyst, *J. Photochem. Photobiol., A*, 325 (2016) 97–103.
- [45] Y. Wu, M. Xing, J. Zhang, F. Chen, Effective visible light-active boron and carbon modified TiO_2 photocatalyst for degradation of organic pollutant, *Appl. Catal., B*, 97 (2010) 182–189.
- [46] N. Chandel, K. Sharma, A. Sudhaik, P. Raizada, A. Hosseini-Bandegharai, V.K. Thakur, P. Singh, Magnetically separable $\text{ZnO}/\text{ZnFe}_2\text{O}_4$ and $\text{ZnO}/\text{CoFe}_2\text{O}_4$ photocatalysts supported onto nitrogen doped graphene for photocatalytic degradation of toxic dyes, *Arabian J. Chem.*, 13 (2020) 4324–4340.
- [47] L. Fernández, M. Gamallo, M.A. González-Gómez, C. Vázquez-Vázquez, J. Rivas, M. Pintado, M.T. Moreira, Insight into antibiotics removal: exploring the photocatalytic performance of a $\text{Fe}_3\text{O}_4/\text{ZnO}$ nanocomposite in a novel magnetic sequential batch reactor, *J. Environ. Manage.*, 237 (2019) 595–608.
- [48] M. Malakootian, H. Mahdizadeh, A. Dehdarirad, M. Amiri Gharghani, Photocatalytic ozonation degradation of ciprofloxacin using ZnO nanoparticles immobilized on the surface of stones, *J. Dispersion Sci. Technol.*, 40 (2019) 846–854.
- [49] M.K. Debanath, S. Karmakar, Study of blueshift of optical band gap in zinc oxide (ZnO) nanoparticles prepared by low-temperature wet chemical method, *Mater. Lett.*, 111 (2013) 116–119.
- [50] S. Narendhran, R. Sivaraj, Biogenic ZnO nanoparticles synthesized using *L. aculeata* leaf extract and their antifungal activity against plant fungal pathogens, *Bull. Mater. Sci.*, 39 (2016) 1–5.
- [51] S. Ahmed, S.A. Chaudhry, S. Ikram, A review on biogenic synthesis of ZnO nanoparticles using plant extracts and microbes: a prospect towards green chemistry, *J. Photochem. Photobiol., B*, 166 (2017) 272–284.
- [52] H. Wang, H. Yao, J. Pei, F. Liu, D. Li, Photodegradation of tetracycline antibiotics in aqueous solution by UV/ ZnO , *Desal. Water Treat.*, 57 (2016) 19981–19987.
- [53] V.H.T. Thi, B.-K. Lee, Great improvement on tetracycline removal using ZnO rod-activated carbon fiber composite prepared with a facile microwave method, *J. Hazard. Mater.*, 324 (2017) 329–339.
- [54] Y.-H. Guan, J. Ma, X.-C. Li, J.-Y. Fang, L.-W. Chen, Influence of pH on the formation of sulfate and hydroxyl radicals in the UV/peroxymonosulfate system, *Environ. Sci. Technol.*, 45 (2011) 9308–9314.
- [55] Y. Chen, C. Hu, J. Qu, M. Yang, Photodegradation of tetracycline and formation of reactive oxygen species in aqueous tetracycline solution under simulated sunlight irradiation, *J. Photochem. Photobiol., A*, 197 (2008) 81–87.
- [56] K.A. Loftin, C.D. Adams, M.T. Meyer, R. Surampalli, Effects of ionic strength, temperature, and pH on degradation of selected antibiotics, *J. Environ. Qual.*, 37 (2008) 378–386.
- [57] C. Zhao, M. Pelaez, X. Duan, H. Deng, K. O’Shea, D. Fatta-Kassinos, D.D. Dionysiou, Role of pH on photolytic and photocatalytic degradation of antibiotic oxytetracycline in aqueous solution under visible/solar light: kinetics and mechanism studies, *Appl. Catal., B*, 134 (2013) 83–92.
- [58] A. Mirzaei, Z. Chen, F. Haghghat, L. Yerushalmi, Removal of pharmaceuticals and endocrine disrupting compounds from water by zinc oxide-based photocatalytic degradation: a review, *Sustainable Cities Soc.*, 27 (2016) 407–418.
- [59] L. Yu, Z. Ye, J. Li, C. Ma, C. Ma, X. Liu, H. Wang, L. Tang, P. Huo, Y. Yan, Photocatalytic degradation mechanism of tetracycline by $\text{Ag}/\text{ZnO}/\text{C}$ core-shell plasmonic photocatalyst under visible light, *Nano*, 13 (2018) 1850065, doi: 10.1142/S1793292018500650.
- [60] F. Guo, W. Shi, W. Guan, H. Huang, Y. Liu, Carbon dots/ $\text{g}-\text{C}_3\text{N}_4/\text{ZnO}$ nanocomposite as efficient visible-light driven photocatalyst for tetracycline total degradation, *Sep. Purif. Technol.*, 173 (2017) 295–303.
- [61] J. Feng, L. Cheng, J. Zhang, O.K. Okoth, F. Chen, Preparation of BiVO_4/ZnO composite film with enhanced visible-light photoelectrocatalytic activity, *Ceram. Int.*, 44 (2018) 3672–3677.
- [62] L. Hu, G. Zhang, M. Liu, Q. Wang, P. Wang, Optimization of the catalytic activity of a ZnCo_2O_4 catalyst in peroxymonosulfate activation for bisphenol A removal using response surface methodology, *Chemosphere*, 212 (2018) 152–161.
- [63] Y. Ding, H. Tang, S. Zhang, S. Wang, H. Tang, Efficient degradation of carbamazepine by easily recyclable microscaled CuFeO_2 mediated heterogeneous activation of peroxymonosulfate, *J. Hazard. Mater.*, 317 (2016) 686–694.
- [64] N.S. Shah, J.A. Khan, M. Sayed, Z.U.H. Khan, A.D. Rizwan, N. Muhammad, G. Boczkaj, B. Murtaza, M. Imran, H.M. Khan, Solar light driven degradation of norfloxacin using as-synthesized Bi^{3+} and Fe^{2+} co-doped ZnO with the addition of HSO_3^- : toxicities and degradation pathways investigation, *Chem. Eng. J.*, 351 (2018) 841–855.
- [65] X. Chen, J. Zhou, T. Zhang, L. Ding, Enhanced degradation of tetracycline hydrochloride using photocatalysis and sulfate radical-based oxidation processes by Co/BiVO_4 composites, *J. Water Process Eng.*, 32 (2019) 100918, doi: 10.1016/j.jwpe.2019.100918.
- [66] Y. Pang, L. Kong, H. Lei, D. Chen, G. Yuvaraja, Combined microwave-induced and photocatalytic oxidation using zinc ferrite catalyst for efficient degradation of tetracycline hydrochloride in aqueous solution, *J. Taiwan Inst. Chem. Eng.*, 93 (2018) 397–404.
- [67] V.M. Mboula, V. Hequet, Y. Gru, R. Colin, Y. Andres, Assessment of the efficiency of photocatalysis on tetracycline biodegradation, *J. Hazard. Mater.*, 209 (2012) 355–364.
- [68] E.F.C. Chauque, J.N. Zvimba, J.C. Ngila, N. Musee, Stability studies of commercial ZnO engineered nanoparticles in domestic wastewater, *Phys. Chem. Earth, Parts A/B/C*, 67 (2014) 140–144.
- [69] V.C. Srivastava, Photocatalytic oxidation of dye bearing wastewater by iron doped zinc oxide, *Ind. Eng. Chem. Res.*, 52 (2013) 17790–17799.
- [70] F. Liu, P. Yi, X. Wang, H. Gao, H. Zhang, Degradation of Acid Orange 7 by an ultrasound/ ZnO -GAC/persulfate process, *Sep. Purif. Technol.*, 194 (2018) 181–187.
- [71] F. Meng, Y. Liu, J. Wang, X. Tan, H. Sun, S. Liu, S. Wang, Temperature dependent photocatalysis of $\text{g}-\text{C}_3\text{N}_4$, TiO_2 and ZnO : differences in photoactive mechanism, *J. Colloid Interface Sci.*, 532 (2018) 321–330.
- [72] R.A. Palominos, M.A. Mondaca, A. Giraldo, G. Peñuela, M. Pérez-Moya, H.D. Mansilla, Photocatalytic oxidation of the antibiotic tetracycline on TiO_2 and ZnO suspensions, *Catal. Today*, 144 (2009) 100–105.
- [73] Y. Qian, G. Xue, J. Chen, J. Luo, X. Zhou, P. Gao, Q. Wang, Oxidation of cefalexin by thermally activated persulfate: kinetics, products, and antibacterial activity change, *J. Hazard. Mater.*, 354 (2018) 153–160.
- [74] R. Xie, J. Ji, K. Guo, D. Lei, Q. Fan, D.Y.C. Leung, H. Huang, Wet scrubber coupled with UV/PMS process for efficient removal of gaseous VOCs: roles of sulfate and hydroxyl radicals, *Chem. Eng. J.*, 356 (2019) 632–640.
- [75] M. Mahdi-Ahmed, S. Chiron, Ciprofloxacin oxidation by UV-C activated peroxymonosulfate in wastewater, *J. Hazard. Mater.*, 265 (2014) 41–46.
- [76] H. Sun, S. Liu, S. Liu, S. Wang, A comparative study of reduced graphene oxide modified TiO_2 , ZnO and Ta_2O_5 in visible light photocatalytic/photochemical oxidation of methylene blue, *Appl. Catal., B*, 146 (2014) 162–168.
- [77] P.R. Shukla, S. Wang, H.M. Ang, M.O. Tadé, Photocatalytic oxidation of phenolic compounds using zinc oxide and sulphate radicals under artificial solar light, *Sep. Purif. Technol.*, 70 (2010) 338–344.
- [78] P. Shukla, I. Fatimah, S. Wang, H.M. Ang, M.O. Tadé, Photocatalytic generation of sulphate and hydroxyl radicals using zinc oxide under low-power UV to oxidise phenolic contaminants in wastewater, *Catal. Today*, 157 (2010) 410–414.

- [79] A. Shad, J. Chen, R. Qu, A.A. Dar, M. Bin-Jumah, A.A. Allam, Z. Wang, Degradation of sulfadimethoxine in phosphate buffer solution by UV alone, UV/PMS and UV/H₂O₂: kinetics, degradation products, and reaction pathways, *Chem. Eng. J.*, 398 (2020) 125357, doi: 10.1016/j.cej.2020.125357.
- [80] L. Duan, B. Sun, M. Wei, S. Luo, F. Pan, A. Xu, X. Li, Catalytic degradation of Acid Orange 7 by manganese oxide octahedral molecular sieves with peroxymonosulfate under visible light irradiation, *J. Hazard. Mater.*, 285 (2015) 356–365.
- [81] J. Chen, J. Xu, T. Liu, Y. Qian, X. Zhou, S. Xiao, Y. Zhang, Selective oxidation of tetracyclines by peroxymonosulfate in livestock wastewater: kinetics and non-radical mechanism, *J. Hazard. Mater.*, 386 (2020) 121656, doi: 10.1016/j.jhazmat.2019.121656.
- [82] C. Wang, J. Jian, Feasibility of tetracycline wastewater degradation by enhanced sonolysis, *J. Adv. Oxid. Technol.*, 18 (2015) 39–46.